Maxwell Garnett theory for mixtures of anisotropic inclusions: Application to conducting polymers

Ohad Levy
Courant Institute of Mathematical Sciences, New York University, New York, New York 10012

David Stroud
Department of Physics, Ohio State University, Columbus, Ohio 43210

(Received 18 February 1997; revised manuscript received 8 May 1997)

The effective dielectric function ϵ_e for a medium of anisotropic inclusions embedded in an isotropic host is calculated using the Maxwell Garnett approximation. For uniaxial inclusions, ϵ_e depends on how well the inclusions are aligned. We apply this approximation to study ϵ_e for a model of quasi-one-dimensional organic polymers. The polymer is assumed to be made up of small single crystals embedded in an isotropic host of randomly oriented polymer chains. The host dielectric function is calculated using the effective-medium approximation (EMA). The resulting frequency-dependent $\epsilon_e(\omega)$ closely resembles experiment. Specifically, $\mathrm{Re}\epsilon_e(\omega)$ is negative over a wide frequency range, while $\mathrm{Im}\epsilon_e(\omega)$ exhibits a broad ''surface plasmon'' band at low frequencies, which results from localized electronic excitations within the crystallites. If the host is above the conductivity percolation threshold, $\mathrm{Im}\epsilon_e(\omega)$ has a low-frequency Drude peak in addition to the surface plasmon band, and $\mathrm{Re}\epsilon_e(\omega)$ is negative over an even wider frequency range. We also calculate the cubic nonlinear susceptibility $\chi_e(\omega)$ of the polymer, using a nonlinear EMA. At certain frequencies, $\chi_e(\omega)$ is found to be strongly enhanced above that of the corresponding single crystals. Our results suggest that the electromagnetic properties of conducting polymers can be understood by viewing the material as randomly inhomogeneous on a small scale such that the quasistatic limit is applicable. [S0163-1829(97)01537-3]

I. INTRODUCTION

The Maxwell Garnett (MG) approximation,[1] also known as the Clausius-Mossotti approximation, is one of the most widely used methods for calculating the bulk dielectric properties of inhomogeneous materials.[2,3] It is useful when one of the components can be considered as a host in which inclusions of the other components are embedded. It involves an exact calculation of the field induced in the uniform host by a single spherical or ellipsoidal inclusion and an approximate treatment of its distortion by the electrostatic interaction between the different inclusions. This distortion is caused by the charge dipoles and higher multipoles induced in the other inclusions. The induced dipole moments cause the longest range distortions and their average effect is included in the MG approximation which results in a uniform field inside all the inclusions. This approach has been extensively used for studying the properties of two-component mixtures in which both the host and the inclusions are isotropic materials with scalar dielectric coefficients. It has also been applied in the study of the Hall effect in inhomogeneous materials, where the components have tensor electrical conductivities under applied magnetic field.[4] In this paper, we present a variation of this approach which is useful for mixtures where the host is an isotropic material but the inclusions are made of anisotropic components.

There are many possible locally anisotropic inhomogeneous materials in which the local dielectric coefficient is a tensor. Of these, the most commonly studied are polycrystalline aggregates of a single anisotropic component.[5,6] In these materials the inhomogeneity is provided by the random variation of the crystal orientation throughout the system. Many of these studies use the effective-medium approximation.[7] This approximation is based on a self-consistent procedure in which a grain of one of the components is assumed to have a convenient shape (usually spherical or ellipsoidal) and to be embedded in an effective medium whose properties are determined self-consistently.[2,8]

In recent years, this approximation has been extensively applied to composites involving high-temperature superconductors. In single-crystal form, such superconductors are highly anisotropic, having conductivities which are much larger in the ab plane than in the third direction. For example, Carr *et al.*[9] and Helsing and Helte[10] have developed slightly different EMA's for mixtures of anisotropic components such that the principal axes of the conductivity tensor of each ellipsoidal crystallite are degenerate with those of the ellipsoid. They have considered models in which the anisotropic grains are randomly oriented, thus leading to an isotropic composite. Walker and Scharnberg[11] have used the model of Ref. 9 to describe the properties of granular superconductors. Diaz-Guilera and Tremblay[12] considered an EMA for mixtures of oriented uniaxial ellipsoids (each with a conductivity matrix degenerate with the axes of the ellipsoid) and an isotropic conductor. This approach differs from the previous models since in this case the composite itself is anisotropic. Genchev[13] applied a similar approach for a mixture of many superconducting components, each distinguished by having a different crystallite shape, and a different conductivity tensor. An extensive EMA study of the optical properties of high-T_c superconductors, modeled as a composite of a uniaxial superconductor and an isotropic normal conductor, has been carried out by Noh *et al.* and by Sulewski *et al.*[14,15]

All these EMA calculations are particularly appropriate for composites and polycrystals in which the grains of the various components are randomly and symmetrically distributed, so that none of the components is identifiable as a host in which the others are preferentially embedded. In this paper, by contrast, we consider a different type of locally anisotropic inhomogeneous materials, made of anisotropic inclusions which are, indeed, randomly embedded in a homogeneous isotropic host. Because of the asymmetry of the assumed geometry, and the approximation, the results are likely to differ somewhat from the symmetric EMA. This geometrical distinction may be easily understood by noting that the EMA and MG approximations are exact for two different microgeometries.[3] The EMA becomes exact in a hierarchical geometry where the two components play symmetrical geometric roles.[16] In contrast, the MG approach is exact for a geometry where the entire space is filled with coated spheres, each with identical ratio of inner to outer radius, such that one component is the core material (isolated inclusions) and the other is the coating material (the host). We consider an example of the later case, with anisotropic inclusions, in which the direction of the dielectric tensor axis may vary from one inclusion to another. The distribution of these directions significantly influences the bulk effective dielectric response of the material and determines its macroscopic anisotropy properties.

In Sec. II, we present an anisotropic version of the MG approximation for the dielectric tensor of such materials. The result obtained depends explicitly on the distribution of crystal orientations inside the inclusions. In Sec. III, we consider anisotropic mixtures in which the local dielectric properties are weakly nonlinear and derive a simple expression for their bulk effective nonlinearity tensor, valid to first order in the local nonlinearity.

In Sec. IV, these results are applied to a simple model of conducting polymers. Heavily doped polymers, such as polyacetylene, polyaniline, and polypyrrole, are quasi-one-dimensional conductors that have attracted considerable interest since the first discovery of electrical conduction in doped polyacetylene.[17] In addition to their interesting conduction properties, these organic polymers usually exhibit relatively large cubic nonlinearity.[18,19] Many papers have discussed possible microscopic mechanisms that may explain these properties. They include exotic elementary excitations such as charged solitons[20] and bipolarons.[21] Typical samples of these materials are collections of crystalline domains, inside which the polymer exhibits three-dimensional order, separated by amorphous regions of the same polymer.[22,23] The crystalline domains are typically ~ 20 Å in diameter and occupy 20–50 % of the material's volume.

This picture suggests that an asymmetric MG theory for anisotropic inclusions in an isotropic matrix may be a reasonable approach to calculate the macroscopic dielectric properties of these disordered polymers. In this paper, rather than discussing microscopic mechanisms, we present a model that may describe how the macroscopic properties of such disordered materials are affected by such a microgeometry. The importance of the microgeometry, and in particular the percolation properties in the presence of inhomogeneous disorder, has been recently demonstrated in experiments on conducting doped polyaniline.[23] Our description includes an explicit connection between the orientational disorder of the crystalline domains, the disorder inside the isotropic host and the macroscopic linear and weakly nonlinear dielectric properties of inhomogeneous conductors.

II. DIELECTRIC RESPONSE OF COMPOSITES WITH ANISOTROPIC INCLUSIONS

Consider a parallel plate condenser whose plates are large enough so that edge effects can be neglected. The condenser is filled by a homogeneous medium with a scalar dielectric constant ϵ_h in which nonoverlapping spheres with a tensor dielectric coefficient $\tilde{\epsilon}_s$ are distributed randomly but uniformly. The orientation of the dielectric tensor differs from inclusion to inclusion, such that

$$\tilde{\epsilon}_s = R\tilde{\epsilon}R^T, \tag{1}$$

where $\tilde{\epsilon}$ is a diagonal tensor and R is the inclusion dependent rotation, which in general depends on the three corresponding Euler angles. Our aim in this section is to derive an expression for the bulk effective dielectric tensor of this mixture.

First we consider a single sphere $\tilde{\epsilon}_s$ immersed in the host ϵ_h. A voltage is applied between the condenser plates such that the volume averaged field in the system is E_0. In this case, the electric field E_s and the displacement field $D_s = \tilde{\epsilon}_s E_s$ inside the inclusion are uniform and satisfy the exact relation[24]

$$D_s + 2\epsilon_h E_s = 3\epsilon_h E_0. \tag{2}$$

The induced dipole moment of the sphere is

$$p_s = V_s \frac{D_s - \epsilon_h E_s}{4\pi} = V_s \frac{3\epsilon_h}{4\pi} \frac{\tilde{\epsilon}_s - \epsilon_h I}{\tilde{\epsilon}_s + 2\epsilon_h I} E_0, \tag{3}$$

where V_s is the volume of the sphere and I is the identity matrix. In this, and in the subsequent equations, the denominators should be understood as representing inverse matrices. From this it follows that if the medium contains a few such spheres, sufficiently far apart for their mutual interactions to be negligible, than the volume averaged polarization in the medium is

$$\langle P \rangle \equiv \frac{1}{V} \sum_s p_s = f \frac{3\epsilon_h}{4\pi} \left\langle \frac{\tilde{\epsilon}_s - \epsilon_h I}{\tilde{\epsilon}_s + 2\epsilon_h I} \right\rangle_R E_0, \tag{4}$$

where f is the volume fraction of the inclusions and $\langle \rangle_R$ denotes an average over the dielectric tensor orientation inside the inclusions.

The bulk effective dielectric tensor can be defined by the ratio between the volume averaged displacement field $D_0 = \langle D \rangle$ and the volume averaged electric field $E_0 = \langle E \rangle$. The volume averaged displacement field is easily calculated by

$$D_0 = \epsilon_h E_0 + 4\pi \langle P \rangle = \left[I + 3f \left\langle \frac{\tilde{\epsilon}_s - \epsilon_h I}{\tilde{\epsilon}_s + 2\epsilon_h I} \right\rangle_R \right] \epsilon_h E_0. \tag{5}$$

The bulk effective dielectric tensor is therefore

$$\tilde{\epsilon}_e = \epsilon_h I + 3f\epsilon_h \left\langle \frac{\tilde{\epsilon}_s - \epsilon_h I}{\tilde{\epsilon}_s + 2\epsilon_h I} \right\rangle_R . \quad (6)$$

This result, ignoring the interaction between the different inclusions, is usually called the dilute limit and is valid only to first order in the volume fraction of the inclusions.

The electrostatic interaction between the inclusions is negligible only in mixtures where their volume fraction is very small. In all other cases it should be taken into account when calculating the dielectric properties of the system. This is most easily done in the MG approximation, where the average field acting on each inclusion is considered to be not the applied field E_0 but the well-known Lorentz local field.[2] Using this correction, the dipolar interaction between the inclusions is taken into account in an averaged way. A simple method to calculate this correction, usually referred to as the excluded volume approach, was proposed by Bragg and Pippard.[25] The average field acting on an inclusion, in a mixture that is not too dense, is the average field in the host medium $E_{\rm ex}$. The difference between $E_{\rm ex}$ and E_0 is due to the correlations between positions of different spheres that arise from the prohibition of overlap between them.[25] Substituting $E_{\rm ex}$ for E_0 in Eq. (2), we find that the field inside the inclusion satisfies the relation

$$D_s + 2\epsilon_h E_s = 3\epsilon_h E_{\rm ex} . \quad (7)$$

The averaged field over the entire system, inside and outside the inclusions, must still be E_0. This leads to a simple relation between the average fields in the host and in the inclusions

$$f\langle E_s \rangle + (1-f\,)E_{\rm ex} = E_0 , \quad (8)$$

where the angular brackets denote a volume average inside the inclusions. Substituting E_s from Eq. (7), we solve for $E_{\rm ex}$ and find

$$E_{\rm ex} = \frac{E_0}{(1-f\,) + 3f\epsilon_h \langle (\tilde{\epsilon}_s + 2\epsilon_h I)^{-1} \rangle_R} . \quad (9)$$

This result can again be used with Eq. (7) to calculate the volume averaged polarization

$$\langle P \rangle = \frac{f}{4\pi} \left\langle \frac{\tilde{\epsilon}_s - \epsilon_h I}{\tilde{\epsilon}_s + 2\epsilon_h I} \right\rangle_R \frac{3\epsilon_h E_0}{(1-f\,) + 3f\epsilon_h \langle (\tilde{\epsilon}_s + 2\epsilon_h I)^{-1} \rangle_R} , \quad (10)$$

which leads to the bulk effective dielectric tensor

$$\tilde{\epsilon}_e = \epsilon_h I + 3f\epsilon_h \left\langle \frac{\tilde{\epsilon}_s - \epsilon_h I}{\tilde{\epsilon}_s + 2\epsilon_h I} \right\rangle_R \times \frac{1}{(1-f\,) + 3f\epsilon_h \langle (\tilde{\epsilon}_s + 2\epsilon_h I)^{-1} \rangle_R} . \quad (11)$$

This is the MG result for mixtures of anisotropic inclusions. It depends on the type of anisotropy of the tensor $\tilde{\epsilon}$ and on the orientation distribution function of the rotation matrices R. As discussed further below, it is not limited to low concentrations of inclusions, but instead is appropriate even at high concentrations, provided that the composite has the assumed geometry (in which a material of one type is embedded in an identifiable host material).

One important example of anisotropic behavior is that of uniaxial materials, where the dielectric coefficient obtains one value along one preferred direction and another value in all perpendicular directions. The dielectric tensor of such a material can be written as

$$\tilde{\epsilon} = \begin{pmatrix} \epsilon_\perp & 0 & 0 \\ 0 & \epsilon_\perp & 0 \\ 0 & 0 & \epsilon_\parallel \end{pmatrix} , \quad (12)$$

in the coordinate system defined by the dielectric axis. For a mixture of many such inclusions, embedded in an isotropic host, it is convenient to define the coordinate system such that the external field E_0 is applied in the positive z direction. The rotation matrix $R = R_{\theta\phi}$ now depends only on two orientation angles θ and ϕ between the principal dielectric axis and the z axis. In this coordinate system the dielectric tensor of each inclusion may be written explicitly as

$$\tilde{\epsilon}_s = R_{\theta\phi} \tilde{\epsilon} R_{\theta\phi}^T = \epsilon_\perp I + \alpha \begin{pmatrix} \cos^2\phi \sin^2\theta & \cos\phi \sin\phi \sin^2\theta & \cos\phi \cos\theta \sin\theta \\ \cos\phi \sin\phi \sin^2\theta & \sin^2\phi \sin^2\theta & \sin\phi \cos\theta \sin\theta \\ \cos\phi \cos\theta \sin\theta & \sin\phi \cos\theta \sin\theta & \cos^2\theta \end{pmatrix} , \quad (13)$$

where $\alpha \equiv \epsilon_\perp - \epsilon_\parallel$. Substituting this in Eq. (11) and defining $\delta \equiv (\epsilon_\perp + 2\epsilon_h)(\epsilon_\parallel - \epsilon_h)$, we find an explicit expression for the bulk effective dielectric tensor, depending on the distribution of the orientation angles θ and ϕ

$$\tilde{\epsilon}_e = \epsilon_h I + \frac{3f\epsilon_h \tilde{A}}{(\epsilon_\perp + 2\epsilon_h)(\epsilon_\parallel + 2\epsilon_h)} \left[1 - f + \frac{3f\epsilon_h \tilde{B}}{(\epsilon_\perp + 2\epsilon_h)(\epsilon_\parallel + 2\epsilon_h)} \right]^{-1} , \quad (14)$$

where

$$\tilde{A} = \begin{pmatrix} \delta - 3\alpha\epsilon_h \langle \cos^2\theta + \sin^2\phi \sin^2\theta \rangle & \frac{3\alpha\epsilon_h}{2} \langle \sin 2\phi \sin^2\theta \rangle & \frac{3\alpha\epsilon_h}{2} \langle \cos\phi \sin 2\theta \rangle \\ \frac{3\alpha\epsilon_h}{2} \langle \sin 2\phi \sin^2\theta \rangle & \delta - 3\alpha\epsilon_h \langle \cos^2\theta + \cos^2\phi \sin^2\theta \rangle & \frac{3\alpha\epsilon_h}{2} \langle \sin\phi \sin 2\theta \rangle \\ \frac{3\alpha\epsilon_h}{2} \langle \cos\phi \sin 2\theta \rangle & \frac{3\alpha\epsilon_h}{2} \langle \sin\phi \sin 2\theta \rangle & \delta + \frac{3\alpha\epsilon_h}{2} (\langle \cos 2\theta \rangle - 1) \end{pmatrix}$$

and

$$\widetilde{B}=\begin{pmatrix} \epsilon_\perp+2\epsilon_h+\alpha\langle\cos^2\theta+\sin^2\phi\ \sin^2\theta\rangle & -\frac{\alpha}{2}\langle\sin2\phi\ \sin^2\theta\rangle & -\frac{\alpha}{2}\langle\cos\phi\ \sin2\theta\rangle \\ -\frac{\alpha}{2}\langle\sin2\phi\ \sin^2\theta\rangle & \epsilon_\perp+2\epsilon_h+\alpha\langle\cos^2\theta+\cos^2\phi\ \sin^2\theta\rangle & -\frac{\alpha}{2}\langle\sin\phi\ \sin2\theta\rangle \\ -\frac{\alpha}{2}\langle\cos\phi\ \sin2\theta\rangle & -\frac{\alpha}{2}\langle\sin\phi\ \sin2\theta\rangle & \frac{\epsilon_\perp+\epsilon_\parallel+4\epsilon_h-\alpha\langle\cos2\theta\rangle}{2} \end{pmatrix}.$$

The angular brackets denote averaging over θ and ϕ of all the inclusions in the mixture.

This result is greatly simplified in cases where these averages can be calculated exactly. Some of these examples are the following.

(1) The dielectric axes of all the inclusions are oriented in the direction of the applied field ($\theta=0$). The effective dielectric tensor in this case is

$$\widetilde{\epsilon}_e=\begin{pmatrix} \epsilon_h+\frac{3f\epsilon_h(\epsilon_\perp-\epsilon_h)}{(\epsilon_\perp-\epsilon_h)(1-f)+3\epsilon_h} & 0 & 0 \\ 0 & \epsilon_h+\frac{3f\epsilon_h(\epsilon_\perp-\epsilon_h)}{(\epsilon_\perp-\epsilon_h)(1-f)+3\epsilon_h} & 0 \\ 0 & 0 & \epsilon_h+\frac{3f\epsilon_h(\epsilon_\parallel-\epsilon_h)}{(\epsilon_\parallel-\epsilon_h)(1-f)+3\epsilon_h} \end{pmatrix}. \tag{15}$$

As expected, this effective dielectric tensor has uniaxial symmetry and its diagonal elements are given by the MG result for isotropic inclusions with dielectric coefficients $\epsilon_\perp$ and $\epsilon_\parallel$, respectively.

(2) The dielectric axes of all the inclusions are oriented in the y direction ($\theta=\pi/2,\ \phi=\pi/2$). The effective dielectric tensor is again uniaxial, but with the MG expression for $\epsilon_\parallel$ inclusions now appearing in the y-axis term instead of in the z-axis term:

$$\widetilde{\epsilon}_e=\begin{pmatrix} \epsilon_h+\frac{3f\epsilon_h(\epsilon_\perp-\epsilon_h)}{(\epsilon_\perp-\epsilon_h)(1-f)+3\epsilon_h} & 0 & 0 \\ 0 & \epsilon_h+\frac{3f\epsilon_h(\epsilon_\parallel-\epsilon_h)}{(\epsilon_\parallel-\epsilon_h)(1-f)+3\epsilon_h} & 0 \\ 0 & 0 & \epsilon_h+\frac{3f\epsilon_h(\epsilon_\perp-\epsilon_h)}{(\epsilon_\perp-\epsilon_h)(1-f)+3\epsilon_h} \end{pmatrix}. \tag{16}$$

A similar result is obtained when all the inclusions are oriented in the x direction ($\theta=\pi/2,\ \phi=0$), by exchanging the x-axis and y-axis terms.

(3) Uniform orientation distribution over $\theta=[0,\pi]$ and $\phi=[0,2\pi]$. It is clear that in this case the entire composite should be isotropic, with a scalar dielectric coefficient. Carrying out the averaging in Eq. (14) we indeed obtain

$$\epsilon_e=\epsilon_h+3f\epsilon_h\frac{(\epsilon_\perp+2\epsilon_h)(\epsilon_\parallel-\epsilon_h)-2\epsilon_h(\epsilon_\parallel-\epsilon_\perp)}{(1-f)(\epsilon_\perp+2\epsilon_h)(\epsilon_\parallel+2\epsilon_h)+f\epsilon_h(\epsilon_\perp+2\epsilon_\parallel+6\epsilon_h)}. \tag{17}$$

Equation (17) is an MG approximation for a volume fraction f of randomly oriented spherical crystallites, each characterized by a uniaxial dielectric tensor, embedded in an isotropic host. It is of interest to contrast this result with approximations, such as that of Ref. 11, in which the randomly oriented anisotropic crystallites and the isotropic component are treated symmetrically. The two approximations do indeed differ: for example, that of Ref. 11 will yield a nonzero percolation threshold for dc conductivity at sufficiently high concentration of anisotropic crystallites, provided that all the principal components of the conductivity tensor of that crystallite are nonzero. By contrast, the MG approximation will always yield a zero dc conductivity of the composite if the host has zero conductivity, because there is no percolation. One cannot say, in general, that one of these approximations is more correct than the other. Instead, the proper choice of an approximation for a given problem depends on which geometry better describes the system of interest. If the geometry is symmetric, the EMA would be more appropriate. In the case of conducting polymers, it appears that the asymmetric geometry is more applicable, and we have therefore adopted the MG approximation in the present work. There is no experimental evidence as for the *shapes* of the polymer inclusions in the materials of interest, thus, rather than making a special assumption, we have simply taken these grain shapes to be spherical.

III. WEAK NONLINEARITY OF ANISOTROPIC COMPOSITES

Quasi-one-dimensional organic polymers sometimes have a remarkably large cubic nonlinear response in the optical regime.[18,19] Enhanced nonlinear properties have been the subject of intense study in other types of disordered structures, e.g., locally isotropic composites consisting of suspensions of nonlinear material in a linear host and layered microstructures of alternating nonlinear dielectrics,[26–35] where it has been demonstrated that the microgeometry greatly contributes to the large effective nonlinearity. The enhancement is produced by a local field effect. The cubic nonlinearity is related to the fourth moment of the local field distribution, and is therefore sensitive to local field values that may be greatly increased above the applied field by fluctuations in the local dielectric properties.

Zeng *et al.*[29] have proposed a method for calculating the effective weak nonlinearity of locally isotropic disordered materials, to first order in the nonlinearity. Here we present a simple generalization of their approach to mixtures of anisotropic components. We consider an anisotropic material, in which the local D and E have a nonlinear relation of the form

$$D_i=\epsilon_{ij}E_j+\chi_{ijkl}E_jE_k^*E_l\,. \tag{18}$$

Here D_i and E_i are the ith Cartesian components of D and E, ϵ_{ij} and χ_{ijkl} are second-rank and fourth-rank Cartesian tensors, and we use the Einstein convention that repeated indices are summed over. The following analysis is carried out in the weakly nonlinear regime, i.e., the nonlinear term is assumed to be small compared to the linear term. We also assume that ϵ_{ij} is symmetric, which insures that it can be diagonalized. For boundary conditions, we consider a sample of volume V, bounded by surface S, on which the potential Φ is specified as $\Phi(x)=-E_0\cdot x$. This choice ensures that the volume average of the electric field within V is E_0. The different elements of the effective dielectric tensor ϵ_e and the cubic nonlinear susceptibility χ_e of the composite may be defined by the relation

$$\langle D_i\rangle=\epsilon_{e;ij}E_{0,i}+\chi_{e;ijkl}E_{0,j}E_{0,k}^*E_{0,l}\,, \tag{19}$$

where $\langle\cdots\rangle$ denotes a volume average. Equivalently, this definition may be written

$$W\equiv V\langle D\rangle\cdot E_0\equiv V[\,\epsilon_{e;ij}E_{0,i}E_{0,j}+\chi_{e;ijkl}E_{0,i}E_{0,j}E_{0,k}^*E_{0,l}], \tag{20}$$

where we have introduced an energylike function W from which ϵ_e and χ_e may be derived.

Note that even though the constitutive relationship (18) is nonlinear and anisotropic, the local fields D and E still satisfy the usual electrostatic equations

$$\nabla\cdot D=0,\quad \nabla\times E=0. \tag{21}$$

From the second of these, E can be expressed as the negative gradient of a scalar potential, $E=-\nabla\Phi$. However, Φ no longer obeys the Laplace equation, because of the complicated (and inhomogeneous) constitutive relation.

The total energy W can also be written as an integral over the local energy, which is

$$W=\int\{\epsilon_{ij}E_iE_j+\chi_{ijkl}E_iE_jE_k^*E_l\}d^3x\equiv W_2+W_4\,. \tag{22}$$

It is easy to prove, from the electrostatic equations (18) and (21) that the definitions (19) and (20) of the effective properties are equivalent. The proof follows closely the analogous proof for isotropic composites.[36] Thus, to determine ϵ_e and χ_e, we need, in principle, only evaluate W for the actual microstructure of the disordered sample, using Eq. (22).

Our first step is to show that to first order in χ_{ijkl}, just as in the isotropic case, χ_e involves the fourth moment of the electric field in a related linear problem. The local electric field may be written as

$$E=E_{\rm lin}+\delta E, \tag{23}$$

where $E_{\rm lin}$ is the electric field that would exist in a linear medium with the same $\epsilon_{ij}(\mathbf{x})$ but with $\chi_{ijkl}(\mathbf{x})=0$, and δE is the additional electric field due to the nonlinearity, which is, by definition, of at least first order in χ_{ijkl}. Since χ_{ijkl} is by assumption a small perturbation on the linear medium, it is sufficient to calculate W only to first order in χ. To this order, we may neglect the contribution of δE to the fourth-order term, since it will only have an effect on W of second order in the χ_{ijkl}'s. The term involving ϵ_{ij} may be written

$$W_2=\int[\,\epsilon_{ij}(E_{{\rm lin};i}+\delta E_i)(E_{{\rm lin};j}+\delta E_j)]d^3x. \tag{24}$$

That portion of W_2 which is first order in δE can be written

$$\delta W_2^{(1)}=\int[2\epsilon_{ij}E_{{\rm lin};i}\delta E_j]d^3x, \tag{25}$$

where we have used the symmetry of ϵ_{ij}. Writing $\delta E_j=-\nabla_j\delta\Phi$ and integrating by parts, we obtain

$$\delta W_2^{(1)}=2\left\{\int[\nabla_j(\epsilon_{ij}E_{{\rm lin};i})\,\delta\Phi]d^3x-\int\nabla_j(\epsilon_{ij}E_{{\rm lin};i}\delta\Phi)d^3x\right\}. \tag{26}$$

But

$$\nabla_j(\epsilon_{ij}E_{{\rm lin};i})=\nabla\cdot D_{\rm lin}=0, \tag{27}$$

where $D_{\rm lin}$ is the displacement vector in the related linear medium, which, like the total displacement D, is divergence free. The integrand of the second term is the divergence of a vector whose jth component is $\epsilon_{ij}E_{{\rm lin};i}\delta\Phi$. Using the divergence theorem, we can convert this integral into a surface integral, which vanishes because $\delta\Phi=0$ on S. Thus $\delta W_2^{(1)}$ vanishes.

The effective coefficients ϵ_e and χ_e are given, according to Eq. (20), by the coefficients of VE_0^2 and VE_0^4 in W. Using the results just proven, we find

$$\epsilon_{e;ij}=\frac{\int\epsilon_{ij}E_{{\rm lin};i}E_{{\rm lin};j}d^3x}{VE_{0,i}E_{0,j}} \tag{28}$$

and

$$\chi_{e;ijkl}=\frac{\int \chi_{ijkl}E_{\mathrm{lin};i}E_{\mathrm{lin};j}E^{*}_{\mathrm{lin};k}E_{\mathrm{lin};l}d^3x}{VE_{0,i}E_{0,j}E^{*}_{0,k}E_{0,l}}. \tag{29}$$

Thus, just as in an isotropic composite, both ϵ_e and χ_e can be expressed (to lowest order in the nonlinearity) in moments of the electric field in the related linear medium. Hereafter, we drop the subscript ''lin;'' only linear fields will be discussed, unless otherwise stated. Denoting the eigenvalues of ϵ_{ij} by ϵ_i and those of $\epsilon_{e;ij}$ by $\epsilon_{e;i}$, we write

$$\epsilon_{e;i}=\frac{\Sigma_\alpha \epsilon_{\alpha;i}\int_\alpha E_i(\mathbf{x})^2 d^3x}{VE^2_{0,i}}, \tag{30}$$

where $E_i(\mathbf{x})$ is the field component parallel to the ith principal axis at $\mathbf{x}$ and the sum is taken over all components α in the mixture. Equation (30) implies that

$$\frac{\langle E_i^2\rangle_\alpha}{E^2_{0,i}}=\frac{1}{p_\alpha}\frac{\partial \epsilon_{e;i}}{\partial \epsilon_{\alpha;i}}, \tag{31}$$

where $\langle\cdots\rangle_\alpha$ denotes a spatial average in the αth component and p_α the volume fraction of that component. This is the analog of a result in isotropic composites,[29]

$$\frac{\langle E^2\rangle_\alpha}{E_0^2}=\frac{1}{p_\alpha}\frac{\partial \epsilon_e}{\partial \epsilon_\alpha}. \tag{32}$$

Considering the nonlinear susceptibility explicitly, we will assume for convenience that, in the body coordinate system, the elements of χ all vanish except χ_{iijj}, with indices equal in pairs. Then from Eq. (29), we get

$$\chi_{e;ij}=\frac{\Sigma_\alpha \chi_{\alpha;iijj}\langle E_i^2|E_j|^2\rangle_\alpha}{E^2_{0;i}|E_{0;j}|^2}. \tag{33}$$

Next, we write down a simple approximation for χ_e analogous to the ''nonlinear decoupling approximation'' (NDA) of isotropic nonlinear composites.[29] The NDA is specified by the assumption that

$$\langle E_i^2|E_j|^2\rangle \approx \langle E_i^2\rangle\langle |E_j|^2\rangle, \tag{34}$$

or, upon using Eqs. (31) and (33),

$$\chi_{e,ij}=\sum_\alpha \frac{\chi_{\alpha;iijj}}{p_\alpha}\left(\frac{\partial \epsilon_{e;i}}{\partial \epsilon_{\alpha;i}}\right)\left|\frac{\partial \epsilon_{e;j}}{\partial \epsilon_{\alpha;j}}\right|. \tag{35}$$

This result is similar to that recently obtained by Stroud[37] for macroscopically isotropic polycrystals of anisotropic materials and is closely analogous to the equation

$$\chi_e=\sum_\alpha \frac{\chi_\alpha}{p_\alpha}\left(\frac{\partial \epsilon_e}{\partial \epsilon_\alpha}\right)^2 \tag{36}$$

which specifies the NDA in mixtures of isotropic components.[29]

Equation (35) is useful given an approximation for the effective dielectric tensor. In our case it can be used together with the MG result (14) to calculate different elements of the effective nonlinearity tensor of the composite.

IV. APPLICATION TO CONDUCTING POLYMERS

As mentioned in the Introduction, typical samples of recently studied conducting polymers are collections of crystalline grains separated by regions of amorphous material, inside which the spatial orientation of the polymer chains changes randomly and continuously.[22,23] Such a structure can be modeled by the MG approach of Sec. II, where the host is not a simple dielectric but is itself a macroscopically isotropic inhomogeneous mixture made of the same anisotropic material as the inclusions. This host may be roughly viewed as a polycrystalline collection of anisotropic, randomly oriented, compact grains much smaller than the spherical inclusions. Its dielectric properties can then be calculated from the principal elements of the local dielectric tensor $\epsilon_\parallel$ and $\epsilon_\perp$ using the well-known effective-medium approximation (EMA). For a locally uniaxial polycrystal, this approximation leads to the simple relation

$$\frac{\epsilon_\parallel-\epsilon_h}{\epsilon_\parallel+2\epsilon_h}+2\frac{\epsilon_\perp-\epsilon_h}{\epsilon_\perp+2\epsilon_h}=0. \tag{37}$$

Solved for ϵ_h, this gives

$$\epsilon_h=\frac{\epsilon_\perp+\sqrt{\epsilon_\perp^2+8\epsilon_\parallel\epsilon_\perp}}{4}, \tag{38}$$

for the dielectric coefficient of the isotropic effective medium. The bulk effective dielectric tensor of the entire system may now be calculated by substituting this result for ϵ_h in Eq. (14).

The EMA of Eq. (38) predicts that the polycrystalline host is precisely at the percolation threshold $p_c=1/3$ of the conducting component $\epsilon_\parallel$. However, it is well known that this approximation predicts too high a threshold for isotropic three-dimensional systems. Thus, it is reasonable to assume that in real samples the conducting component does percolate inside the isotropic host. This expected behavior can be mimicked within our model by introducing an effective ''volume fraction'' p higher than $p_c=1/3$ in the effective-medium expression (37) for ϵ_h

$$p\frac{\epsilon_\parallel-\epsilon_h}{\epsilon_\parallel+2\epsilon_h}+(1-p)\frac{\epsilon_\perp-\epsilon_h}{\epsilon_\perp+2\epsilon_h}=0. \tag{39}$$

In a mixture of two isotropic components, p would be the volume fraction of the component with dielectric constant $\epsilon_\parallel$. In our model, however, the material is a collection of randomly oriented polymer chains, and the concept of a volume fraction has no clear definition. Instead it should be viewed as a measure of the connectivity of the component $\epsilon_\parallel$. In highly disordered samples, the polymer chains are relatively short. This leads to short continuous paths of $\epsilon_\parallel$, only a few of which will connect opposite sides of the entire system. This low connectivity corresponds to a small value of p. By contrast, in samples with lower disorder the polymer chains are longer, on average, and create more extended continuous paths of $\epsilon_\parallel$. These samples will have relatively many paths of $\epsilon_\parallel$ which span the entire system, and therefore higher connectivity and a larger effective value of p. While the best choice of p is difficult to fix, we believe that this equation does describe the real physical behavior of the host,

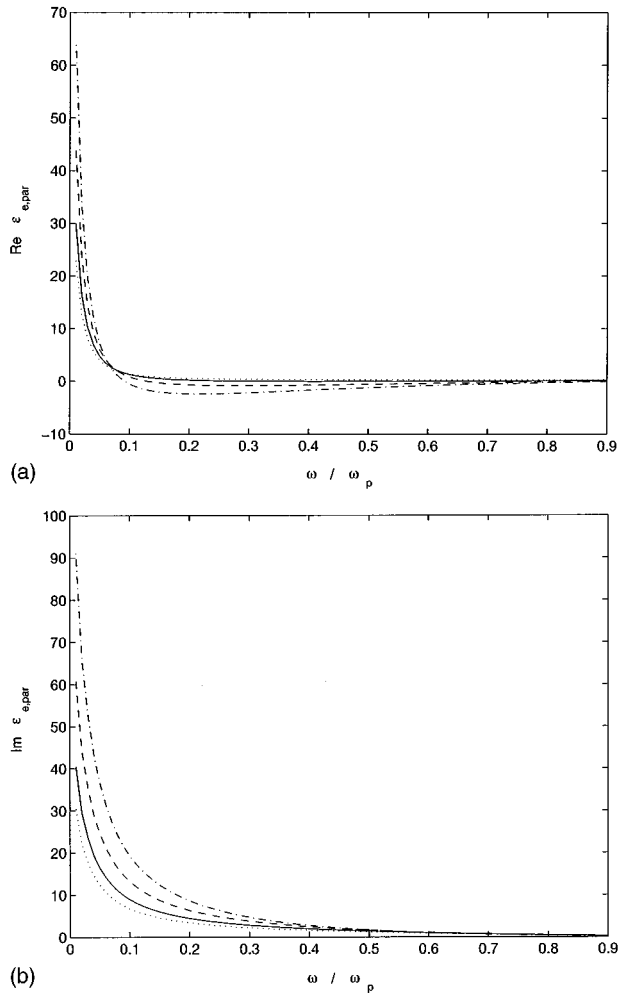

FIG. 1. Real and imaginary parts of the component parallel to the applied field of the effective dielectric tensor for a mixture of aligned inclusions, Eq. (15). Results are shown for $\omega_p\tau=30$ in the metallic direction and $f=0.1$ (solid line), $f=0.25$ (dashed line), and $f=0.4$ (dash-dotted line). The dotted line is the corresponding result for a mixture of randomly oriented inclusions, Eq. (17).

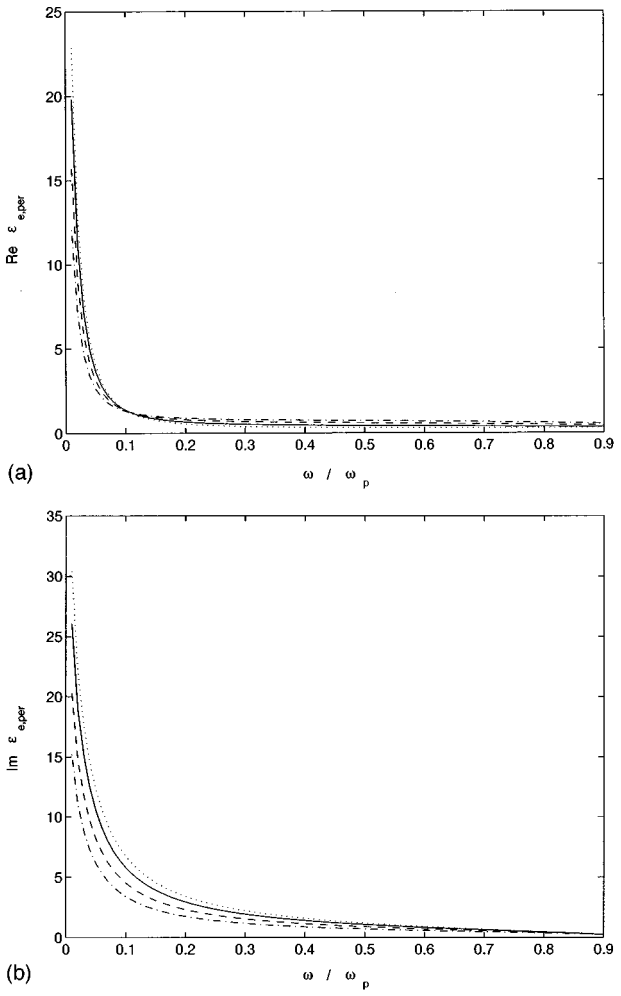

FIG. 2. Real and imaginary parts of the component perpendicular to the applied field of the effective dielectric tensor of Eq. (15). The different curves are as in Fig. 1.

namely, that it is a random amorphous collection of polymer chains in which there may be infinite connected (percolating) paths of the polymer in the high-conductivity direction.

A. Linear dielectric response

To illustrate the predicted dielectric behavior for the simple examples of Sec. II A, we consider a highly simplified model of a quasi-one-dimensional conductor. In the high-conductivity direction we assume a Drude metal with dielectric function

$$\epsilon_{\parallel}(\omega)=1-\omega_p^2/[\omega(\omega+i/\tau)]. \tag{40}$$

In the perpendicular direction, we assume simply an insulator with

$$\epsilon_{\perp}(\omega)=1. \tag{41}$$

Numerical results for aligned and randomly oriented inclusions, with $\omega_p\tau=30$, embedded in a host ϵ_h of Eq. (38) [or of Eq. (39) with $p=1/3$] are shown in Figs. 1 and 2. In Fig. 1(a) we plot the real part of the parallel component of Eq. (15) for three different volume fractions of the spherical inclusions. As the volume fraction of the oriented inclusions increases the influence of the metallic behavior along their principal axis becomes more pronounced. This leads to the appearance of a frequency range, below ω_p, where the real part of the dielectric coefficient is negative. This range widens, and the dielectric coefficient becomes more negative, as the volume fraction increases. The imaginary part, shown in Fig. 1(b), increases with volume fraction, as the metallic behavior becomes more important. The results are markedly different for the perpendicular component of Eq. (15). The conducting direction plays a much smaller role in this case and the real part of ϵ_e is never negative. Its trend of change, as the volume fraction increases, is opposite to that of the parallel component [see Fig. 2(a)]. The imaginary part, shown in Fig. 2(b), now decreases with volume fraction, as the influence of the high conductivity direction becomes less pronounced.

In mixtures of randomly oriented inclusions and a host exactly at the percolation threshold (38), the bulk effective dielectric coefficient does not depend on the volume fraction [results for this case are shown for reference in Figs. (1) and (2) (dotted lines)]. This can be shown by a direct calculation that leads to

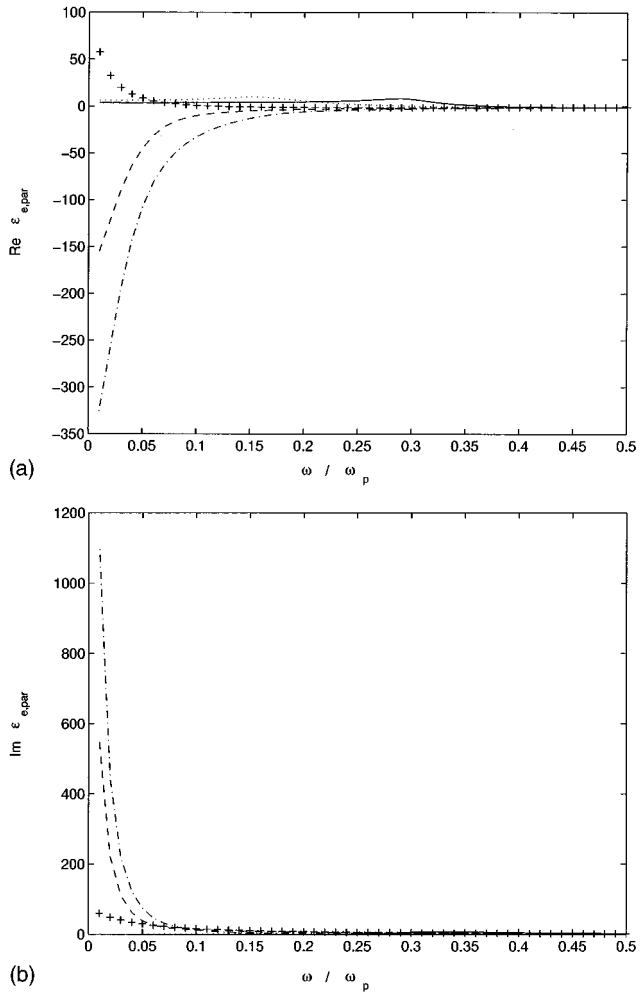

FIG. 3. Real and imaginary parts of the component parallel to the applied field of the effective dielectric tensor for a mixture of aligned inclusions, Eq. (15). Results are shown for $\omega_p\tau=30$ in the metallic direction, $f=1/3$ and $p=0.1$ (solid line), $p=0.2$ (dotted line), $p=0.33$ (crosses), $p=0.4$ (dashed line), and $p=0.5$ (dash-dot line). The imaginary part for the two lowest values of p are indistinguishable from the x axis.

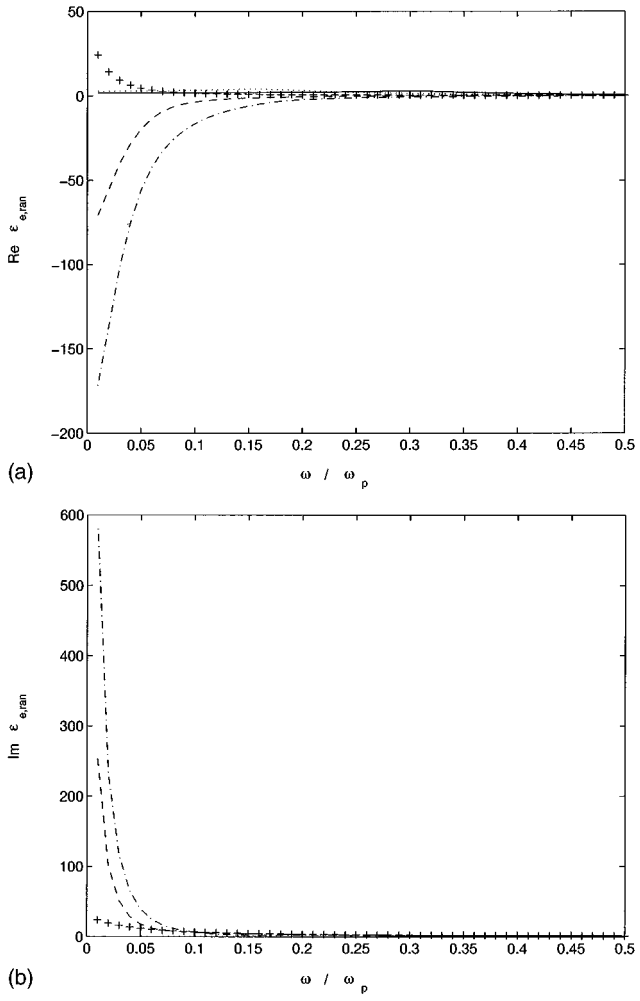

FIG. 4. Real and imaginary parts of the effective dielectric constant for mixtures of randomly oriented inclusions, Eq. (17). The different curves are for different values of p as in Fig. 4.

$$\left\langle \frac{\tilde{\epsilon}_s-\epsilon_h I}{\tilde{\epsilon}_s+2\epsilon_h I}\right\rangle_{\theta\phi}=\frac{(\epsilon_\perp+2\epsilon_h)(\epsilon_\parallel-\epsilon_h)-2\epsilon_h(\epsilon_\parallel-\epsilon_\perp)}{(\epsilon_\perp+2\epsilon_h)(\epsilon_\parallel+2\epsilon_h)}$$

$$=\frac{1}{3}\frac{\epsilon_\parallel-\epsilon_h}{\epsilon_\parallel+2\epsilon_h}+\frac{2}{3}\frac{\epsilon_\perp-\epsilon_h}{\epsilon_\perp+2\epsilon_h}=0, \qquad (42)$$

where the last equality is obtained from Eq. (37). Substituting this in Eq. (11) we again get $\tilde{\epsilon}_e=\epsilon_h I$ with ϵ_h given by Eq. (38). This result is intuitively obvious, since the collection of randomly oriented inclusions is macroscopically equivalent to the polycrystalline host ϵ_h of Eq. (38). This is not the case in any mixture where the host is not exactly at the percolation threshold, since the exact equivalence between the collection of randomly oriented inclusions and the host no longer holds. In all of these cases, the entire material must be isotropic with a scalar bulk effective dielectric coefficient.

Results for different values of connectivity p, both above and below the percolation threshold, are shown in Figs. 3 and 4. In Fig. 3(a) we plot the real part of the parallel component of Eq. (15) (inclusions aligned parallel to the applied field) for five different values of p, with the same volume fraction of the inclusions $f=1/3$. The results show a qualitatively different behavior above and below the percolation threshold $p_c=1/3$. Below p_c, the real part of ϵ_e is positive, and relatively small, in the entire range of frequencies below ω_p. Above p_c, a zero crossing appears below which $\mathrm{Re}\epsilon_e$ is negative. This zero crossing occurs at higher frequencies for higher values of $p>p_c$ ($\omega/\omega_p=0.89$ for $p=0.4$ and $\omega/\omega_p=0.93$ for $p=0.5$). This behavior follows qualitatively experimental results on conducting polymers in which high conductivity samples exhibit zero crossing and negative $\mathrm{Re}\epsilon_e$ at low frequencies.[22,23] Low conductivity samples, on the other hand, have positive $\mathrm{Re}\epsilon_e$ at all frequencies. The imaginary part of ϵ_e, Fig. 3(b), increases at low frequencies as p increases. $\mathrm{Im}\epsilon_e$ of low conductivity samples $p<p_c$ is indistinguishable from the x axis at the entire range of frequencies below ω_p. But in high conductivity samples where $p>p_c$, it is enhanced at low frequencies by two or three orders of magnitude. Similar behavior is obtained for mixtures of randomly oriented inclusions, Fig. 4. As expected, the effects of varying the value of p are somewhat less significant than in the aligned inclusions case. The range of frequencies at

which $\mathrm{Re}\epsilon_e$ is negative for $p>p_c$ is smaller and the negative values obtained are also smaller. The zero crossing points are now $\omega/\omega_p=0.31$ for $p=0.4$ and $\omega/\omega_p=0.48$ for $p=0.5$. The enhancement of $\mathrm{Im}\epsilon_e$ at low frequencies is still significant but not as large as for aligned inclusions. Even weaker effects, although with the same general trend, are obtained in mixtures with inclusions aligned perpendicular to the applied field. This behavior is a result of the reduced importance of the metallic component $\epsilon_\parallel$ in these cases compared to mixtures where it is aligned parallel to the field.

In Figs. 3 and 4, $\mathrm{Re}\epsilon_e$ of the high conductivity samples crosses the x axis at a single frequency, below which it is negative. Experimental studies on polyaniline and polypyrrole have shown that under certain circumstances $\mathrm{Re}\epsilon_e$ may exhibit *three* zero crossings instead of one, leading to *two* separate frequency bands where it is negative.[22,23] One band appears at very low frequencies, as in Figs. 3 and 4, and the other at slightly higher frequencies. Between these two bands $\mathrm{Re}\epsilon_e$ is relatively large and positive. These observations suggest that the metallic behavior of the polymer, along its principal axis, is somewhat more complicated than the simple Drude behavior of Eq. (40).

As a simple model for this behavior, we add to the Drude dielectric function an additional ''vibrational'' contribution at a finite frequency ω_0. This leads to a dielectric coefficient of the form

$$\epsilon_\parallel(\omega)=1-\frac{\omega_p^2}{\omega(\omega+i/\tau)}+\frac{\omega_s^2}{\omega_0^2-\omega^2-i\gamma\omega}, \tag{43}$$

where the amplitude ω_s, the resonant frequency ω_0 and the damping constant γ are material dependent constants. Substituting this $\epsilon_\parallel$, and retaining the polycrystalline host of Eq. (39), in Eq. (14) indeed leads to $\mathrm{Re}\epsilon_e$ with three zero crossings for all three different distributions of inclusion orientations discussed above.

In Figs. 5 and 6 we show results from this model, for inclusions aligned parallel to the applied field and for randomly oriented inclusions. In each plot, the individual curves represent different values of p used in Eq. (39) for the host dielectric function. The two negative $\mathrm{Re}\epsilon_e$ bands are clearly apparent in the high conductivity cases ($p>p_c=1/3$). In addition to the low frequency band of Figs. 3 and 4, we now get a higher band from the vibrational contribution of Eq. (43). Between the bands, $\mathrm{Re}\epsilon_e$ attains large positive values in qualitative agreement with experiments. These bands do not appear in low conductivity samples, where the host is either at or below p_c, and $\mathrm{Re}\epsilon_e$ never crosses the x axis. The vibrational contribution also leads to a local maximum of $\mathrm{Im}\epsilon_e$ at the frequencies of the higher band. As in Figs. 3 and 4, the bands are wider, and $\mathrm{Re}\epsilon_e$ is more negative, when the inclusions are aligned. Similar, but weaker, behavior is again obtained for inclusions aligned perpendicular to the field. These results show that our macroscopically disordered structural model can easily reproduce the experimentally observed dielectric response of conducting polymers.

B. Weak cubic nonlinearity

In this section we apply the results of Secs. II and III to demonstrate that the special microgeometry of conducting polymers may play an important role in their relatively large nonlinear dielectric properties. As shown in Sec. III, the elements of the effective nonlinearity tensor of anisotropic mixtures can be calculated from the simple relation (35). This result may be further simplified for our model of conducting polymers, since the disorder in it originates from the different spatial organization of a single uniaxial component in different regions inside the system and not from mixing a few different components. Therefore, in this case, the sum over the different components can be dropped from Eq. (35) and we are thus left with a simple relation that depends only on the eigenvalues of the local dielectric tensor

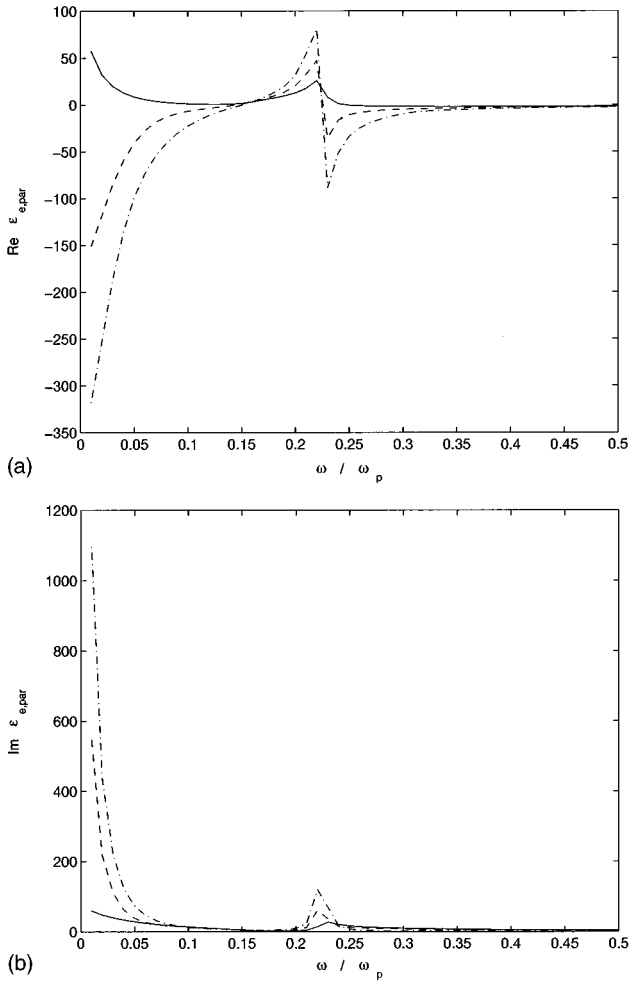

FIG. 5. Real and imaginary parts of $\epsilon_{e,\parallel}$ of Eq. (15), using Eq. (43) for $\epsilon_\parallel$ and Eq. (39) for ϵ_h. Results are shown for $\omega_p\tau=30$, $\omega_s^2=1$, $\omega_0^2=0.05$, $\gamma=0.01$, $f=1/3$ and $p=1/3$ (solid line), $p=0.4$ (dashed line), and $p=0.5$ (dash-dotted line).

$$\chi_{e;ij}=\chi_{iijj}\left(\frac{\partial\epsilon_{e;i}}{\partial\epsilon_i}\right)\left|\frac{\partial\epsilon_{e;j}}{\partial\epsilon_j}\right|, \tag{44}$$

where χ_e is the bulk effective nonlinearity tensor, χ is the anisotropic local nonlinearity tensor, and ϵ_i,ϵ_j are eigenvalues of the anisotropic local dielectric coefficient. In the examples discussed in this paper, these two eigenvalues are $\epsilon_\parallel$ and $\epsilon_\perp$. As in Sec. III, it is assumed here that in the body coordinate system the elements of χ all vanish except χ_{iijj}, with indices equal in pairs.

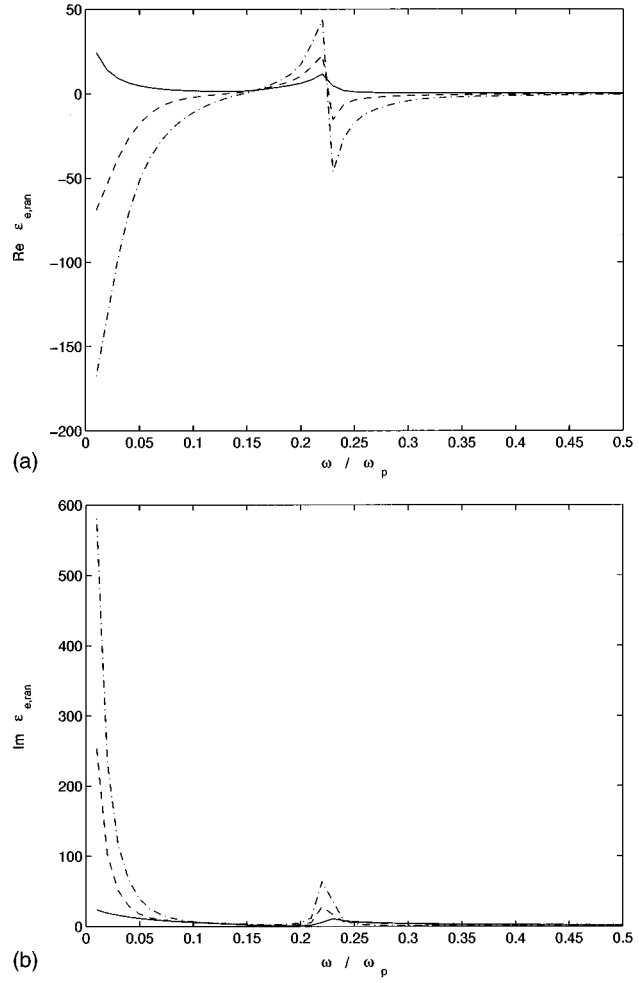

FIG. 6. Real and imaginary parts of ϵ_e for mixtures of randomly oriented inclusions, Eq. (17), with Eq. (43) for $\epsilon_\parallel$ and Eq. (39) for ϵ_h. The different lines are for different values of p as in Fig. 6.

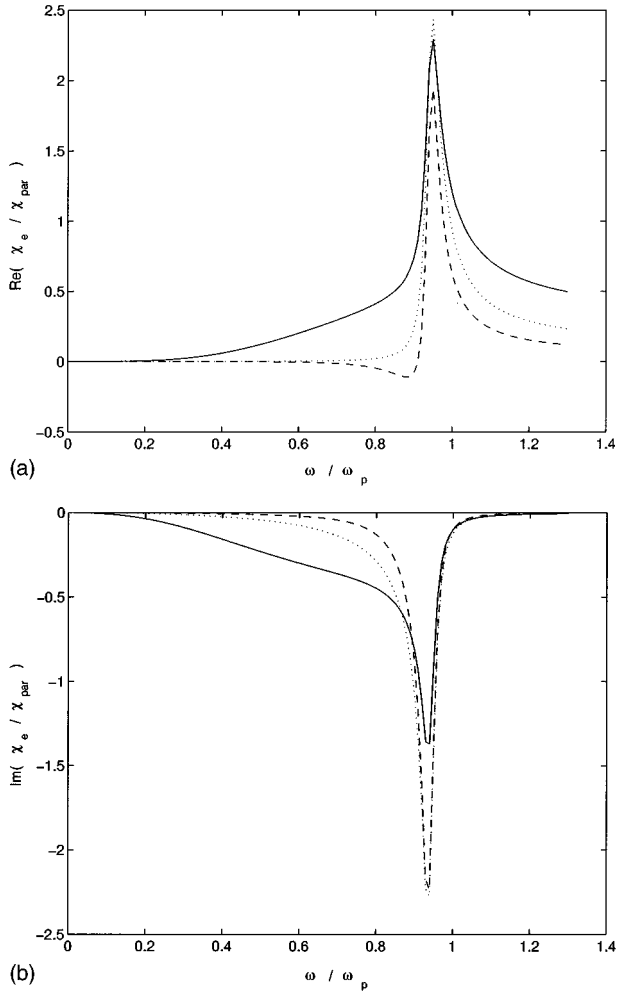

FIG. 7. Real and imaginary parts of the nonlinearity coefficient for a mixture where only $\chi_{\rm par}=\chi_{\parallel,\parallel}\neq 0$. Shown are results derived from the component parallel (solid line) and perpendicular (dashed line) to the applied field of Eq. (15), and the dielectric coefficient of a mixture of randomly oriented inclusions, Eq. (17) (dotted line) with a polycrystalline host of Eq. (38).

To apply this approximation to the examples discussed in Sec. II A, we solve Eq. (14) for ϵ_e and compute the specified derivatives. Examples are shown for inclusions aligned parallel (solid curve) and perpendicular (dashed curve) to the applied field and for randomly oriented inclusions (dotted line). The results for different combinations of χ_{iijj}, with volume fraction $f=1/3$, are shown in Figs. 7–9. In Fig. 7 it is assumed that only $\chi_{\rm par}=\chi_{\parallel,\parallel}\neq 0$. Results for the case where only $\chi_{\rm per}=\chi_{\perp,\perp}\neq 0$ are shown in Fig. 8, and results for $\chi_{\rm mix}=\chi_{\parallel,\perp}\neq 0$ are shown in Fig. 9. Clearly, whichever component of χ is nonzero, χ_e is substantially enhanced at appropriate frequencies. In this approximation, the low-frequency enhancement of $\chi_{\rm per}$ in particular is huge. The physical origin of this enhancement is a large increase in local electric fields at the interface between the inclusions and the isotropic host. The uniaxial (high-dielectric-constant) direction predominates in carrying displacement current inside the inclusions. But within the EMA, the host is exactly at the percolation threshold for carrying displacement current. The MG approximation then predicts a large local field enhancement in the low-conductivity crystal directions. Therefore, χ_e, which depends on the fourth power of the local electric field, is greatly increased. The enhancement would be larger in systems where the contrast between $\epsilon_\parallel$ and $\epsilon_\perp$ is larger. It would be smaller for examples were the isotropic host is taken to be above the percolation threshold [such as in Eq. (39)] and in cases where the contrast between $\epsilon_\parallel$ and $\epsilon_\perp$ is smaller.

V. DISCUSSION

We now consider to what extent our results may be consistent with experimental observations on various quasi-one-dimensional conducting polymers. Kohlman *et al.*[22,23] have recently studied the dielectric response of polypyrrole and polyaniline over a broad range of frequencies from the microwave to the optical. Many of the observed features closely resemble those found here. For example, at high frequencies, they find that $\mathrm{Re}\epsilon_e(\omega)$ is positive, with a Drude-like frequency dependence. As the frequency is reduced, they observe a zero crossing followed by a broad frequency range in which $\mathrm{Re}\epsilon_e(\omega)$ is negative. At still lower frequencies, there is generally a second zero crossing below which $\mathrm{Re}\epsilon_e(\omega)$ is

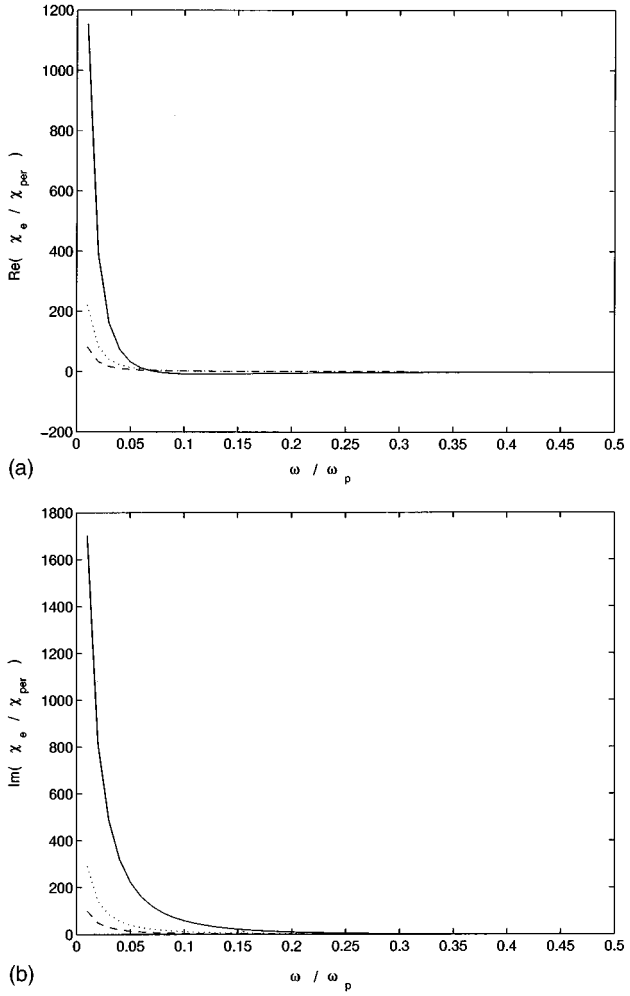

FIG. 8. Real and imaginary parts of the nonlinearity coefficient for a mixture where only $\chi_{\rm per}=\chi_{\perp,\perp}\neq 0$. The different curves are derived from different effective dielectric coefficients as in Fig. 7.

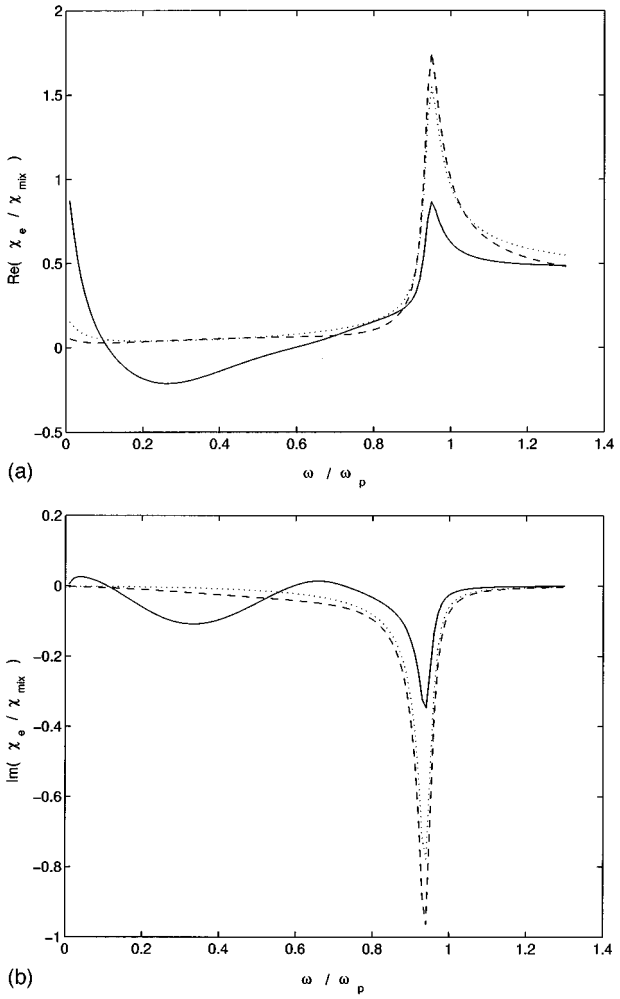

FIG. 9. Real and imaginary parts of the nonlinearity coefficient for a mixture where only $\chi_{\rm mix}=\chi_{\parallel,\perp}\neq 0$. The different curves are as in Fig. 7.

again positive. Finally, at the lowest frequencies studied, $\mathrm{Re}\epsilon_e(\omega)$ shows a behavior which seems to depend on the dc conductivity of the polymer: the low-conductivity samples have a positive dielectric constant, while those with highest conductivity have $\mathrm{Re}\epsilon_e(\omega)$ large and negative.

Our results show similar behavior, and also depend in similar way on the dc conductivity. For example, when we have a host which is at or below percolation, $\mathrm{Re}\epsilon_e(\omega)$ is positive at low frequencies, while for an above-percolation host, $\mathrm{Re}\epsilon_e(\omega)$ is negative over a broad low-frequency range, in agreement with experiments on polypyrrole and polyaniline.[22,23] These results confirm, in agreement with experiment, that $\mathrm{Re}\epsilon_e(\omega)$ should be strongly dependent on the microstructure of the polymer system.

Our composite results also exhibit a characteristic broad surface plasmon peak in $\mathrm{Im}\epsilon_e(\omega)$. This peak, which extends down to very low frequencies, arises in this model from localized oscillations of the charge carriers in one or a few crystallites of polymer; the carriers are localized because of the disordered microstructure (which is characterized by a spatially varying dielectric tensor). Such a peak is typical of conducting polymers, where it has been attributed to both composite effects[22,23,38] and to Anderson localization.[39] The present results support the idea that this band in the dielectric response may be due simply to the inhomogeneity of the polymer medium, without invoking quantum localization.

The extension of our model to the nonlinear susceptibility is less easily tested, at present, because the χ tensor for single crystals of conducting polymers may not be known. In addition, our results depend somewhat on the validity of the nonlinear EMA used in Sec. III, which is not well established. Nevertheless, the model certainly does suggest a mechanism for a large χ in conducting polymers. An experiment to measure the frequency dependence of χ, and possibly to detect the peaks seen in Figs. 7–9, would be most desirable.

Finally, we briefly comment on the long-wavelength assumption which underlies our treatment of both linear and nonlinear response in the polycrystal. This assumption means that the crystallite size should be small with respect to both the wavelength of the electromagnetic field in the medium, and to the electromagnetic skin depth. For wavelengths of interest (in the visible and below), this assumption should be very well satisfied for grains of size smaller than 200–300 Å. In the far infrared, in the most conducting samples, there might be some absorption arising from eddy currents associated with induced magnetic dipoles in the

small particles. These are not included in our quasistatic approximation which assumes $\nabla \times \mathbf{E} = 0$ (see, for example, Ref. 3).

In summary, we have described a Maxwell Garnett approximation to treat $\epsilon_e(\omega)$ for a suspension of quasi-one-dimensional crystallites in an isotropic host. The model leads to a macroscopic dielectric behavior which qualitatively agrees with experiments on polypyrrole and polyaniline, and accounts for the dependence of ϵ_e on the static electrical conductivity. An extension of the model also provides a mechanism for a large enhancement of the cubic nonlinear susceptibility of conducting polymers.

ACKNOWLEDGMENTS

We are grateful for useful conversations with A. J. Epstein, A. Kazaryan, and R. V. Kohn. This work was supported by NSF Grant No. DMS-9402763 and ARO Grant No. DAAH04-95-1-0100 (O.L.) and by NSF Grant No. DMR 94-02131 (D.S.).

[1] J. C. M. Garnett, Philos. Trans. R. Soc. London, Ser. B **203**, 385 (1904).
[2] R. Landauer, in *Electrical Transport and Optical Properties of Inhomogeneous Media*, edited by J. C. Garland and D. B. Tanner, AIP Conf. Proc. No. 40 (AIP, New York, 1978).
[3] D. J. Bergman and D. Stroud, Solid State Phys. **46**, 147 (1992).
[4] D. Stroud and F. P. Pan, Phys. Rev. B **13**, 1434 (1976).
[5] M. Avellaneda, A. V. Cherkaev, K. A. Lurie, and G. W. Milton, J. Appl. Phys. **63**, 4989 (1988), and references therein.
[6] M. Avellaneda and O. Bruno, J. Math. Phys. (N.Y.) **31**, 2047 (1990).
[7] D. A. G. Bruggeman, Ann. Phys. (Leipzig) **24**, 636 (1935).
[8] R. Landauer, J. Appl. Phys. **23**, 779 (1952).
[9] G. L. Carr, S. Perkowitz, and D. B. Tanner, in *Infrared and Millimeter Waves*, edited by K. J. Button (Academic Press, London, 1985), Vol. 13.
[10] J. Helsing and A. Helte, J. Appl. Phys. **69**, 3583 (1991).
[11] D. Walker and K. Scharnberg, Phys. Rev. B **42**, 2211 (1990).
[12] A. Diaz-Guilera and A.-M. S. Tremblay, J. Appl. Phys. **69**, 379 (1991).
[13] Z. D. Genchev, Supercond. Sci. Technol. **6**, 532 (1992).
[14] T. W. Noh, P. W. Sulewski, and A. J. Sievers, Phys. Rev. B **36**, 8866 (1987).
[15] P. E. Sulewski, T. W. Noh, J. T. McWhirter, and A. J. Sievers, Phys. Rev. B **36**, 5735 (1987).
[16] G. W. Milton, in *The Physics and Chemistry of Porous Media*, D. L. Johnson and P. N. Sen, AIP Conf. Proc. No. 107 (AIP, New York, 1983).
[17] *Handbook of Conducting Polymers*, edited by T. A. Skotheim (Dekker, New York, 1986).
[18] *Nonlinear Optical Properties of Organic and Polymeric Materials*, ACS Symp. Series No. 233, edited by David J. Williams (American Chemical Society, Washington, D.C., 1983).
[19] *Organic Materials for Nonlinear Optics*, edited by R. Hann and D. Bloor (Royal Society of Chemistry, London, 1989), Vols. I and II.
[20] A. J. Heeger, S. Kivelson, J. R. Schrieffer, and W. P. Su, Rev. Mod. Phys. **60**, 781 (1988).
[21] A. J. Epstein, H. Rommermann, R. Bigelow, H. W. Gibson, D. M. Hoffman, and D. B. Tanner, Phys. Rev. Lett. **50**, 1866 (1983).
[22] R. S. Kohlman, J. Joo, Y. Z. Wang, J. P. Pouget, H. Kaneko, T. Ishiguro, and A. J. Epstein, Phys. Rev. Lett. **74**, 773 (1995).
[23] R. S. Kohlman, J. Joo, Y. G. Min, A. G. MacDiarmid, and A. J. Epstein, Phys. Rev. Lett. **77**, 2766 (1996).
[24] L. D. Landau, E. M. Lifshitz, and L. P. Pitaevskii, *Electrodynamics of Continuous Media*, 2nd ed. (Pergamon Press, New York, 1984), Chap. II.
[25] W. L. Bragg and A. B. Pippard, Acta Crystallogr. **6**, 865 (1953).
[26] A short review is given in Ref. 3, pp. 246–258.
[27] D. Ricard, in *Nonlinear Optics: Materials and Devices*, edited by C. Flytzanis and J. L. Oudar (Springer-Verlag, Berlin, 1986).
[28] D. Stroud and Van E. Wood, J. Opt. Soc. Am. B **6**, 778 (1989).
[29] X. C. Zeng, D. J. Bergman, P. M. Hui, and D. Stroud, Phys. Rev. B **38**, 10 970 (1988); X. C. Zeng, P. M. Hui, D. J. Bergman, and D. Stroud, Physica A **157**, 192 (1989).
[30] D. Ricard, Physica A **157**, 301 (1989).
[31] J. W. Haus, N. Kalyaniwalla, R. Inguva, M. Bloemer, and C. M. Bowden, J. Opt. Soc. Am. B **6**, 797 (1989).
[32] O. Levy and D. J. Bergman, Phys. Rev. B **46**, 7189 (1992).
[33] J. E. Sipe and R. W. Boyd, Phys. Rev. A **46**, 1614 (1992).
[34] O. Levy and D. J. Bergman, Physica A **191**, 475 (1992).
[35] G. L. Fischer, R. W. Boyd, R. J. Gehr, S. A. Jenekhe, J. A. Osaheni, J. E. Sipe, and L. A. Weller-Brophy, Phys. Rev. Lett. **74**, 1871 (1995).
[36] D. Stroud and P. M. Hui, Phys. Rev. B **37**, 8719 (1988).
[37] D. Stroud, Phys. Rev. B **54**, 3295 (1996).
[38] D. Stroud and A. Kazaryan, Phys. Rev. B **53**, 7076 (1996).
[39] K. Lee, A. J. Heeger, and Y. Cao, Phys. Rev. B **48**, 14 884 (1993); M. Reghu, C. O. Yoon, D. Moses, A. J. Heeger, and Y. Cao, *ibid.* **48**, 17 685 (1993).